North American tree migration paced by climate in the West, lagging in the East

Shubhi Sharma, Robert Andrus, Yves Bergeron, Michal Bogdziewicz, Don Bragg, Dale Brockway, Natalie Cleavitt, Benoît Courbaud, Adrian Das, Michael Dietze, et al.

▶ **To cite this version:**

Shubhi Sharma, Robert Andrus, Yves Bergeron, Michal Bogdziewicz, Don Bragg, et al.. North American tree migration paced by climate in the West, lagging in the East. Proceedings of the National Academy of Sciences of the United States of America, 2022, 119 (3), pp.1-9. 10.1073/pnas.2116691118 . hal-04032657

HAL Id: hal-04032657
https://hal.inrae.fr/hal-04032657v1

Submitted on 19 Jan 2024

HAL is a multi-disciplinary open access archive for the deposit and dissemination of scientific research documents, whether they are published or not. The documents may come from teaching and research institutions in France or abroad, or from public or private research centers.

L'archive ouverte pluridisciplinaire **HAL**, est destinée au dépôt et à la diffusion de documents scientifiques de niveau recherche, publiés ou non, émanant des établissements d'enseignement et de recherche français ou étrangers, des laboratoires publics ou privés.

Distributed under a Creative Commons Attribution - NonCommercial - NoDerivatives 4.0 International License

ETH zürich

ETH Library

North American tree migration paced by climate in the West, lagging in the East

Journal Article

Author(s):
Sharma, Shubhi; Andrus, Robert; Bergeron, Yves; Bogdziewicz, Michal; Bragg, Don C.; Brockway, Dale; Cleavitt, Natalie L.; Courbaud, Benoît; Das, Adrian J.; Dietze, Michael; Fahey, Timothy J.; Franklin, Jerry F.; Gilbert, Gregory S.; Greenberg, Cathryn H.; Guo, Qinfeng; Hille Ris Lambers, Janneke; Ibanez, Ines; Johnstone, Jill F.; Kilner, Christopher L.; Knops, Johannes M.H.; Koenig, Walter D.; Kunstler, Georges; LaMontagne, Jalene M.; Macias, Diana; Moran, Emily; Myers, Jonathan A.; Parmenter, Robert; Pearse, Ian S.; Poulton-Kamakura, Renata; Redmond, Miranda D.; Reid, Chantal D.; Rodman, Kyle C.; Scher, C. Lane; Schlesinger, William H.; Steele, Michael A.; Stephenson, Nathan L.; Swenson, Jennifer J.; Swift, Margaret; Veblen, Thomas T.; Whipple, Amy V.; Whitham, Thomas G.; Wion, Andreas P.; Woodall, Christopher W.; Zlotin, Roman; Clark, James S.

Publication date:
2022-01-18

Permanent link:
https://doi.org/10.3929/ethz-b-000529018

Rights / license:
Creative Commons Attribution-NonCommercial-NoDerivatives 4.0 International

Originally published in:
Proceedings of the National Academy of Sciences of the United States of America 119(3), https://doi.org/10.1073/pnas.2116691118

This page was generated automatically upon download from the ETH Zurich Research Collection.
For more information, please consult the Terms of use.

North American tree migration paced by climate in the West, lagging in the East

Shubhi Sharma[a], Robert Andrus[b], Yves Bergeron[c], Michal Bogdziewicz[d], Don C. Bragg[e], Dale Brockway[f], Natalie L. Cleavitt[g], Benoit Courbaud[h], Adrian J. Das[i], Michael Dietze[j], Timothy J. Fahey[g], Jerry F. Franklin[k], Gregory S. Gilbert[l], Cathryn H. Greenberg[m], Qinfeng Guo[n], Janneke Hille Ris Lambers[o], Ines Ibanez[p], Jill F. Johnstone[q], Christopher L. Kilner[a], Johannes M. H. Knops[r], Walter D. Koenig[s], Georges Kunstler[h], Jalene M. LaMontagne[t], Diana Macias[u], Emily Moran[v], Jonathan A. Myers[w], Robert Parmenter[x], Ian S. Pearse[y], Renata Poulton-Kamakura[a], Miranda D. Redmond[z], Chantal D. Reid[a], Kyle C. Rodman[aa], C. Lane Scher[a], William H. Schlesinger[a], Michael A. Steele[bb], Nathan L. Stephenson[i], Jennifer J. Swenson[a], Margaret Swift[a], Thomas T. Veblen[b], Amy V. Whipple[cc], Thomas G. Whitham[cc], Andreas P. Wion[z], Christopher W. Woodall[dd], Roman Zlotin[ee,ff], and James S. Clark[a,h,1]

[a]Nicholas School of the Environment, Duke University, Durham, NC 27708; [b]Department of Geography, University of Colorado, Boulder, CO 80309; [c]Forest Research Institute, University of Quebec in Abitibi-Temiscamingue, Rouyn-Noranda, QC J9X 5E4, Canada; [d]Department of Systematic Zoology, Faculty of Biology, Adam Mickiewicz University, 61-614 Poznan, Poland; [e]Southern Research Station, US Department of Agriculture Forest Service, Monticello, AR 71656; [f]Southern Research Station, US Department of Agriculture Forest Service, Auburn, AL 36849; [g]Natural Resources, Cornell University, Ithaca, NY 14853; [h]Universite Grenoble Alpes, Laboratoire EcoSystemes et Societes En Montagne, Institut National de Recherche pour Agriculture, Alimentation, et Environnement, 38402 St. Martin-d'Heres, France; [i]Western Ecological Research Center, US Geological Survey, Three Rivers, CA 93271; [j]Earth and Environment, Boston University, Boston, MA 02215; [k]Forest Resources, University of Washington, Seattle, WA 98195; [l]Department of Environmental Studies, University of California, Santa Cruz, CA 95064; [m]Bent Creek Experimental Forest, US Department of Agriculture Forest Service, Asheville, NC 28801; [n]Eastern Forest Environmental Threat Assessment Center, Southern Research Station, US Department of Agriculture Forest Service, Research Triangle Park, NC 27709; [o]Department of Environmental Systems Science, Eidgenössische Technische Hochschule Zurich, Zurich 8092, Switzerland; [p]School for Environment and Sustainability, University of Michigan, Ann Arbor, MI 48109; [q]Institute of Arctic Biology, University of Alaska, Fairbanks, AK 99700; [r]Health and Environmental Sciences Department, Xian Jiaotong-Liverpool University, Suzhou 215123, China; [s]Hastings Reservation, University of California Berkeley, Carmel Valley, CA 93924; [t]Department of Biological Sciences, DePaul University, Chicago, IL 60614; [u]Department of Biology, University of New Mexico, Albuquerque, NM 87131; [v]School of Natural Sciences, University of California, Merced, CA 95343; [w]Department of Biology, Washington University in St. Louis, St. Louis, MO 63130; [x]Valles Caldera National Preserve, National Park Service, Jemez Springs, NM 87025; [y]Fort Collins Science Center, US Geological Survey, Fort Collins, CO 80526; [z]Department of Forest and Rangeland Stewardship, Colorado State University, Fort Collins, CO 80523; [aa]Department of Forest and Wildlife Ecology, University of Wisconsin-Madison, Madison, WI 53706; [bb]Department of Biology, Wilkes University, Wilkes-Barre, PA 18766; [cc]Department of Biological Sciences, Northern Arizona University, Flagstaff, AZ 86011; [dd]Forest Inventory and Analysis, US Forest Service, Durham, NH 03824; [ee]Geography Department, Indiana University, Bloomington, IN 47405; and [ff]Russian and East European Institute, Indiana University, Bloomington, IN 47405

Contributed by James S. Clark; received September 14, 2021; accepted November 22, 2021; reviewed by Amy Angert and Thomas Wohlgemuth

Tree fecundity and recruitment have not yet been quantified at scales needed to anticipate biogeographic shifts in response to climate change. By separating their responses, this study shows coherence across species and communities, offering the strongest support to date that migration is in progress with regional limitations on rates. The southeastern continent emerges as a fecundity hotspot, but it is situated south of population centers where high seed production could contribute to poleward population spread. By contrast, seedling success is highest in the West and North, serving to partially offset limited seed production near poleward frontiers. The evidence of fecundity and recruitment control on tree migration can inform conservation planning for the expected long-term disequilibrium between climate and forest distribution.

climate change | forest regeneration | seed production | tree migration

Effective planning for the redistribution of habitats from climate change will depend on understanding demographic rates that control population spread at continental scales. Mobile species are moving, some migrating poleward (1, 2) and/or upward in elevation (3, 4). Species redistribution is also predicted for sessile, long-lived trees that provide the resource and structural foundation for global forest biodiversity (5–7), but their movement is harder to study. Contemporary range shifts are recognized primarily where contractions have followed extensive die-backs (8) or where local changes occur along compact climate gradients in steep terrain (9, 10). Whether migration capacity can pace habitat shifts of hundreds of kilometers on decade time scales depends on seed production and juvenile recruitment (Fig. 1*A*), which have not been fitted to data in ways that can be incorporated in models to anticipate biogeographic change (11–13). For example, do the regions of rapid warming coincide with locations where species can produce abundant seed (Fig. 1*B*)? If so, does seed production translate to juvenile recruitment? Here, we combine continent-wide fecundity

Significance

Suitable habitats for forest trees may be shifting fast with recent climate change. Studies tracking the shift in suitable habitat for forests have been inconclusive, in part because responses in tree fecundity and seedling establishment can diverge. Analysis of both components at a continental scale reveals a poleward migration of northern species that is in progress now. Recruitment and fecundity both contribute to poleward spread in the West, while fecundity limits spread in the East, despite a fecundity hotspot in the Southeast. Fecundity limitation on population spread can confront conservation and management efforts with persistent disequilibrium between forest diversity and rapid climate change.

Author contributions: J.S.C. designed research; S.S., R.A., Y.B., M.B., D.C.B., D.B., N.L.C., B.C., A.J.D., M.D., T.J.F., J.F.F., G.S.G., C.H.G., Q.G., J.H.R.L., I.I., J.F.J., C.L.K., J.M.H.K., W.D.K., G.K., J.M.L., D.M., E.M., J.A.M., R.P., I.S.P., R.P.-K., M.D.R., C.D.R., K.C.R., C.L.S., W.H.S., M.A.S., N.L.S., J.J.S., M.S., T.T.V., A.V.W., T.G.W., A.P.W., C.W.W., R.Z., and J.S.C. performed research; J.S.C. contributed new reagents/analytic tools; S.S. and J.S.C. analyzed data; and S.S. and J.S.C. wrote the paper.

Reviewers: A.A., University of British Columbia; T.W., Swiss Federal Research Institute WSL.

Competing interest statement: M.B., W.D.K., and I.S.P. are collaborators on a 2020 review with T.W.

This article is distributed under Creative Commons Attribution-NonCommercial-NoDerivatives License 4.0 (CC BY-NC-ND).

[1]To whom correspondence may be addressed. Email: jimclark@duke.edu.

This article contains supporting information online at https://www.pnas.org/lookup/suppl/doi:10.1073/pnas.2116691118/-/DCSupplemental.

Published January 10, 2022.

Downloaded from https://www.pnas.org by ETH Bibliothek on May 13, 2022 from IP address 129.132.180.126.

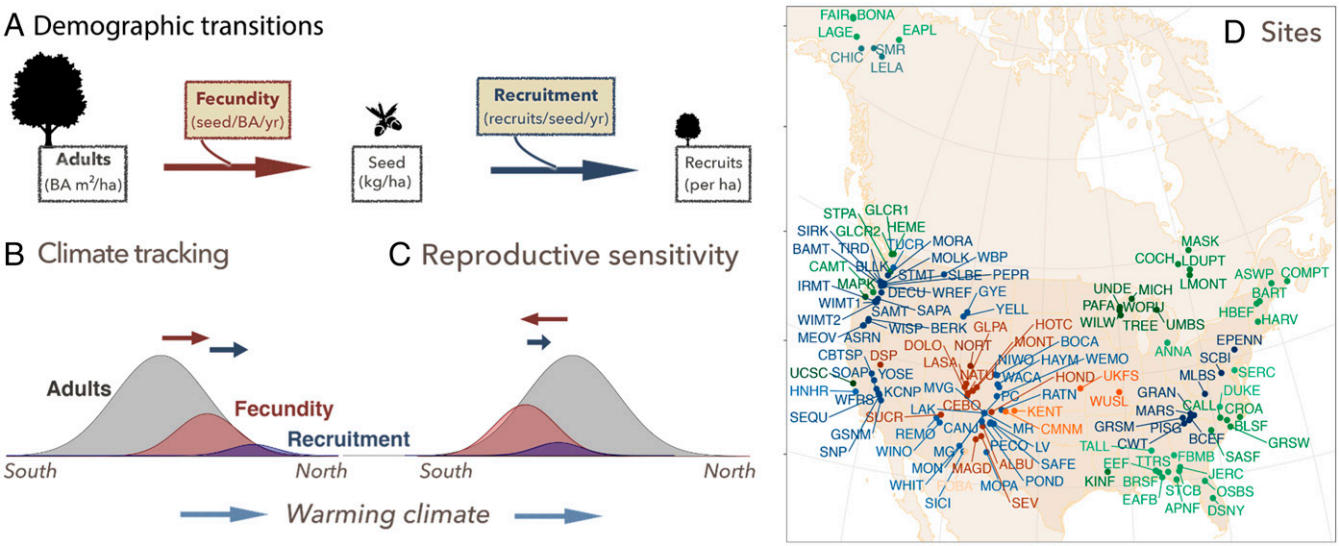

Fig. 1. Transitions, hypothesized effects on spread, and sites. (*A*) Population spread from trees (BA) to new recruits is controlled by fecundity (seed mass per BA) followed by recruitment (recruits per seed mass). (*B*) The CTH that warming has stimulated fecundity ahead of the center of adult distributions, which reflect climate changes of recent decades. Arrows indicate how centroids from trees to fecundity to recruitment could be displaced poleward with warming climate. (*C*) The RSH that cold-sensitive fecundity is optimal where minimum temperatures are warmer than for adult trees and, thus, may slow northward migration. The two hypotheses are not mutually exclusive. *B* and *C* refer to the probability densities of the different life stages. (*D*) MASTIF sites are summarized in *SI Appendix*, Table S2.2 by eco-regions: mixed forest (greens), montane (blues), grass/shrub/desert (browns), and taiga (blue-green).

estimates from the Masting Inference and Forecasting (MASTIF) network (13) with tree inventories to identify North American hotspots for recruitment and find that species are well-positioned to track warming in the West and North, but not in parts of the East.

Suitable habitats for many species are projected to shift hundreds of kilometers in a matter of decades (14, 15). While climate effects on tree mortality are increasingly apparent (16–19), advances into new habitats are not (20–23). For example, natural populations of *Pinus taeda* may be sustained only if the Northeast can be occupied as habitats are lost in the South (Fig. 2). Current estimates of tree migration inferred from geographic comparisons of juvenile and adult trees have been inconclusive (2, 7, 21, 24, 25). Ambiguous results are to

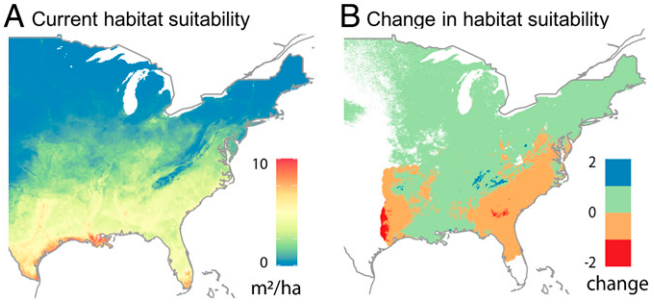

Fig. 2. Suitable habitats redistribute with decade-scale climate change for *P. taeda* (BA units m^2 /ha). (Suitability is not a prediction of abundance, but rather, it is defined for climate and habitat variables included in a model, to be modified by management and disturbance [e.g., fire]. By providing habitat suitability in units of BA, it can be related it to the observation scale for the data.) Predictive distributions for suitability under current (*A*) and change expected from mid-21st-century climate scenario Representative Concentration Pathway 4.5 (*B*) showing habitat declines in the Southwest and East. Specific climate changes important for this example include net increases in aridity in the southeast (especially summer) and western frontier and warming to the North. Occupation of improving habitats depends on fecundity in northern parts of the range and how it is responding. Obtained with Generalized Joint Attribute Modeling (see *Materials and Methods* for more information).

be expected if fecundity and juvenile success do not respond to change in the same ways (20, 26–29). Moreover, seedling abundances (7, 30) do not provide estimates of recruitment rates because seedlings may reside in seedling banks for decades, or they may turn over annually (31–33). Another method based on geographic shifts in population centers calculated from tree inventories (3, 34) does not separate the effects of mortality from recruitment, i.e., the balance of losses in some regions against gains in others. The example in Fig. 2 is consistent with an emerging consensus that suitable habitats are moving fast (2, 14, 15), even if population frontiers are not, highlighting the need for methods that can identify recruitment limitation on population spread. Management for forest products and conservation goals under transient conditions can benefit from an understanding of recruitment limitation that comes from seed supply, as opposed to seedling survival (35).

We hypothesized two ways in which fecundity and recruitment could slow or accelerate population spread. Contemporary forests were established under climates that prevailed decades to centuries ago. These climate changes combine with habitat variables to affect seeds, seedlings, and adults in different ways (36, 37). The "climate-tracking hypothesis" (CTH) proposes that, after decades of warming and changing moisture availability (Fig. 3 *A* and *B*), seed production for many species has shifted toward the northern frontiers of the range, thus primed for poleward spread. "Fecundity," the transition from tree basal area (BA) to seed density on the landscape (Fig. 1*A*), is taken on a mass basis (kg/m^2 BA) as a more accurate index of reproductive effort than seed number (38, 39). "Recruitment," the transition from seed density to recruit density (recruits per kg seed), may have also shifted poleward, amplifying the impact of poleward shifts in fecundity on the capacity for poleward spread (Fig. 1*B*). Under CTH, the centers for adult abundance, fecundity, and recruitment are ordered from south to north in Fig. 1*B* as might be expected if each life-history stage leads the previous stage in a poleward migration.

The "reproductive-sensitivity hypothesis" (RSH) proposes that recruitment may limit population growth in cold parts of the range (Fig. 1*C*), where fecundity and/or seedling survival is already low. Cold-sensitive reproduction in plants includes

Downloaded from https://www.pnas.org by ETH Bibliothek on May 13, 2022 from IP address 129.132.180.126.

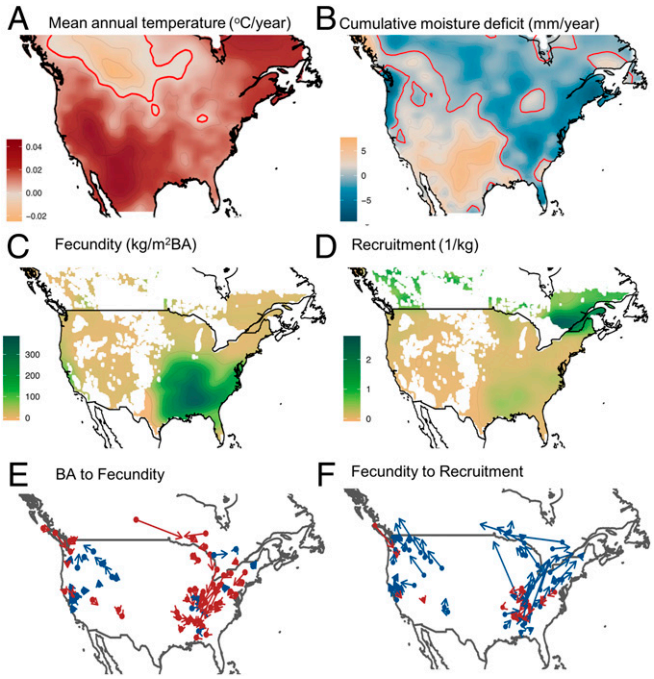

Fig. 3. Climate change and tracking. (*A*) Mean annual temperatures since 1990 have increased rapidly in the Southwest and much of the North. (Zero-change contour line is in red.) (*B*) Moisture deficit index (monthly potential evapotranspiration minus P summed over 12 mo) has increased in much of the West. (Climate sources are listed in *SI Appendix*.) (*C*) Fecundity (kg seed per BA summed over species) is high in the Southeast. (*D*) Recruits per kg seed (square-root transformed) is highest in the Northeast. (*E* and *F*) Geographic displacement of 81 species show transitions in Fig. 1*A*, as arrows from centroids for adult BA to fecundity (*E*) and from fecundity to recruitment (*F*). Blue arrows point north; red arrows point south. Consistent with the RSH (Fig. 1*B*), most species centered in the East and Northwest have fecundity centroids south of adult distributions (red arrows in *E*). Consistent with the CTH, species of the interior West have fecundity centroids northwest of adults (blue arrows). Recruitment is shifted north of fecundity for most species (blue arrows in *F*). *SI Appendix*, Fig. S2 shows that uncertainty in vectors is low.

late frost that can disrupt flowering, pollination, and/or seed development, suggesting that poleward population frontiers tend to be seed-limited (40–44). While climate warming could reduce the negative impacts of low temperatures, especially at northern frontiers, these regions still experience the lowest temperatures. The view of cold-sensitive fecundity as a continuing rate-limiting step, i.e., that has not responded to warming in Fig. 1*C*, is intended to contrast with the case where warming has alleviated temperature limitation in Fig. 1*B*. Lags can result if cold-sensitive recruitment naturally limits growth at high-latitude/high-altitude population frontiers (Fig. 1*C*). In this case, reproductive sensitivity may delay the pace of migration to an extent that depends on fecundity, recruitment, or both at poleward frontiers. The arrows in Fig. 1*C* depict a case where optimal fecundity is equator-ward of optimal growth and recruitment. The precise location of recruitment relative to fecundity in Fig. 1*C* will depend on all of the direct and indirect effects of climate, including through seed and seedling predators and disturbances like fire. Fig. 1*C* depicts one of many hypothetical examples to show that climate variables might have opposing effects on fecundity and recruitment.

Both CTH and RSH can apply to both temperature and moisture; the latter is here quantified as cumulative moisture deficit between potential evapotranspiration and precipitation, $D = \sum_{m=1}^{12}(PET_m - P_m)$ for month m, derived from the widely used Standardized Precipitation Evapotranspiration Index (45). Whereas latitude dominates temperature gradients and longitude is important for moisture in the East, gradients are complicated by steep terrain in the West, with temperature tending to decline and moisture increase with elevation.

We quantified the transitions that control population spread, from adult trees (BA) to fecundity (seeds per BA) to recruitment (recruits per kg seed) (Fig. 1*A*–*C*). Fecundity observations are needed to establish the link between trees and recruits in the migration process. They must be available at the tree scale across the continent because seed production depends on tree species and size, local habitat, and climate for all of the dominant species and size classes (13, 46). These estimates are not sufficient in themselves, because migration depends on seed production per area, not per tree. The per-area estimates come from individual seed production and dispersal from trees on inventory plots that monitor all trees that occupy a fixed sample area. Fecundity estimates were obtained in the MASTIF project (13) from 211,000 (211K) individual trees and 2.5 million (2.5M) tree-years from 81 species. We used a model that accommodates individual tree size, species, and environment and the codependence between trees and over time (Fig. 1*C*). In other words, it allows valid inference on fecundity, the quasisynchronous, quasiperiodic seed production typical of many species (47). The fitted model was then used to generate a predictive distribution of fecundity for each of 7.6M trees on 170K forest inventory plots across the United States and Canada. Because trees are modeled together, we obtain fecundity estimates per plot and, thus, per area. BA (m^2 /ha) of adult trees and new recruits into the smallest diameter class allowed us to determine fecundity as kg seed per m^2 BA and recruitment per kg seed, i.e., each of the transitions in Fig. 1*A*.

Recruitment rates, rather than juvenile abundances, come from the transitions from seedlings to sapling stages. The lag between seed production and recruitment does not allow for comparisons on an annual basis; again, residence times in a seedling bank can span decades. Instead, we focus on geographic variation in mean rates of fecundity and recruitment.

We summarized the geographic distributions for each transition as 1) the mean transition rates across all species and 2) the geographic centroids (central tendency) for each species as weighted-average locations, where weights are the demographic transitions (BA to fecundity, fecundity to recruitment, and BA to recruitment). We analyzed central tendency, or centroids (e.g., refs. 3 and 34) because range limits cannot be accurately identified on the basis of small inventory plots (21). If fecundity is not limiting poleward spread (CTH of Fig. 1*B*), then fecundity centroids are expected to be displaced poleward from the adult population. If reproductive sensitivity dominates population spread (RSH of Fig. 1*C*), then fecundity and/or recruitment centroids will be displaced equator-ward from adult BA. The same comparisons between fecundity and recruitment determine the contribution of recruitment to spread.

Results

Geographic centroids for demographic rates show a biogeographic divide in their support for the two hypotheses. Taken over all species, the analysis identified distinct geographic centers for fecundity and recruitment and coherent geographic shifts across stage transitions. A fecundity hotspot occupies the warm, moist southeastern continent, across the Piedmont Plateau and southern Interior Highlands and, secondarily, in Mediterranean California (Fig. 3*C*). In the East, the fecundity centroids for species that contribute to this hotspot are shifted south from BA centroids of the same species (red arrows in Fig. 3*E*). This is a region of modest warming (Fig. 3*A*), which might contribute to the lack of poleward displacement of fecundity. The north–south gradient in moisture change (Fig. 3*B*) may have limited influence if moisture limitation does not strongly impact average

Downloaded from https://www.pnas.org by ETH Bibliothek on May 13, 2022 from IP address 129.132.180.126.

fecundity in the humid East [it certainly does affect interannual and intersite variability (26, 43)].

The pattern of vectors in eastern forests (Fig. 3) is consistent with the RSH, i.e., fecundity displaced south of adult populations and toward the fecundity hotspot of the Southeast and Interior Highlands (red arrows in Fig. 3*E*)—the region where warming has been comparatively slow (Fig. 3*A*). This southward displacement of fecundity is also observed in the Pacific Northwest and desert Southwest. By contrast, the interior West shows fecundity centroids shifted northwest of tree BA, consistent with the CTH (blue arrows in Fig. 3*E*).

The east–west contrast in tree BA-to-fecundity transitions is emphasized by plotting the vectors from Fig. 3 *E* and *F* onto a common origin in Fig. 4 *A* and *B*. The mixture of influences in the mountain and coastal West (Fig. 4*A*) is expected if responses include local elevation gradients, a contrast with the strong south and west displacement of fecundity in the East (Fig. 4*B*). If moisture has a strong effect on fecundity centroids in the interior West, then combined increases in temperature and moisture deficits (Fig. 3 *A* and *B*) may explain fecundity shifts toward moist, cool climates that prevail northwest of adult centroids.

The east–west fecundity differences are only weakly related to the climates that species currently occupy. The perspective of climate space (as opposed to geographic space) shows that some species having BA centered in cool/moist climates tend to have fecundity offset toward warmer/drier climates and vice versa (Fig. 4*C*). Western species account for both the lowest and highest spring temperature centroids (Fig. 4*D*). A tendency for arrows to point centrally in Fig. 4 *C* and *D* is expected if fecundity represents the sensitive life-history stage in both regions, but this trend is not ubiquitous.

The distinct east–west contrast disappears at the second-stage transition from fecundity to recruitment (Fig. 3 *D* and *F*). By contrast with fecundity, the recruitment hotspot occurs in the North and only secondarily in the Southeast. Conifer-dominated northern forests (*Pinus*, *Abies*, and *Picea*) show the highest recruits per kg seed (Fig. 3*D*) in regions where climate has become increasingly wetter and warmer. With the exception of some species in the Southeast (red in Fig. 3*F*) and in the coastal Pacific Northwest, recruitment is everywhere shifted poleward (blue in Fig. 3*F*), indicating that seedling establishment is responding to warming faster than fecundity. This displacement of recruitment centroids occurs in the direction of not only higher temperature, but also higher moisture (Fig. 3 *A* and *B*)—vectors point northeast in the East and northwest in the intermountain West (Fig. 3*F*). The contrast between fecundity and recruitment provides strong evidence that fecundity represents the more cold-sensitive stage, on average, and lower sensitivity of juvenile stages may tend to compensate for the effects on fecundity. The fact that both sides of the continent show the geographic shift toward moist climates is consistent with the interpretation of moisture-limited recruitment in warming climates, even in the relatively moist East. Exceptions in the East (red arrows in the southeast of Fig. 3*F*) include species centered where climates are geographically complicated by the southern Appalachian mountains.

Net migration combines fecundity and juvenile success to produce a north–south biogeographic response that is distinct from its two components (Fig. 4*E*). While lack of northward spread for species centered in the Southeast is consistent both with the RSH and limited warming there (compare Figs. 3*E* and 4*E*), recruitment compensates for fecundity limitation in the Northeast, but it is dominated by an eastward trend. Again, while slow spread in the Southeast coincides with a region of limited warming, it does not by itself explain the dominant southward displacement of fecundity from adult population centers, a pattern that is

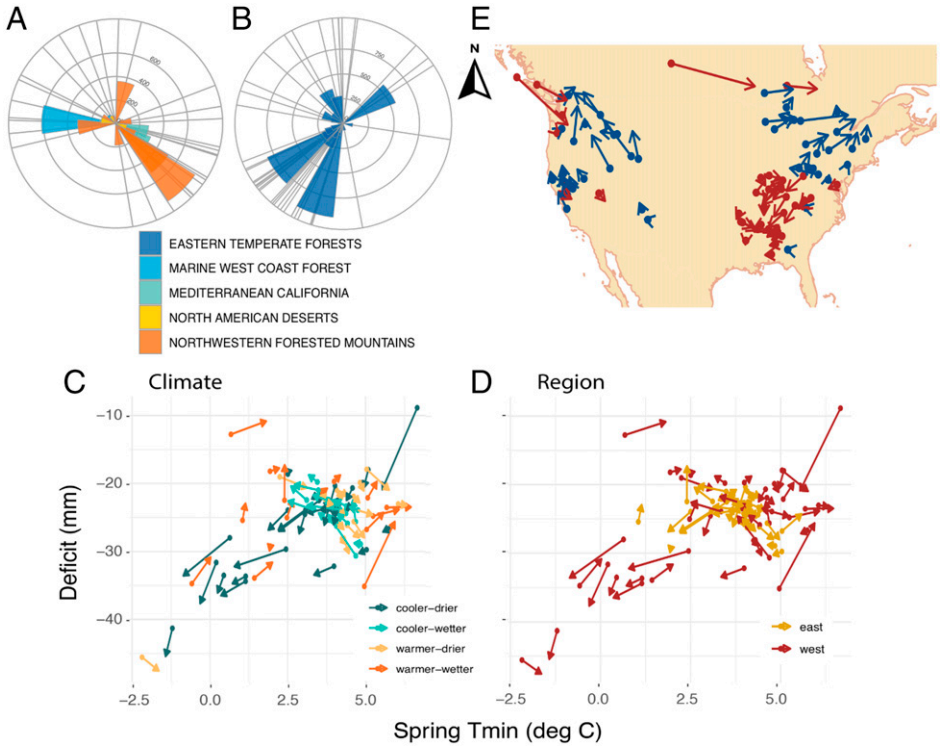

Fig. 4. Fecundity vectors from Fig. 3*E* compare distance/direction for west (*A*) and east (*B*) by ecoregion. Radial bars are centered at BA centroids and connecting to fecundity centroids, with radial distance given in km. *C* and *D* locate the same vectors in climate space (spring minimum temperatures and summer moisture deficit), colored by directions in climate space and geographic space, respectively. (*E*) Geographic displacement of 81 species between adult BA centroid (filled circles) to recruitment centroid. Blue arrows point north; red arrows point south. The dominant pattern in the west is northward-pointing arrows, consistent with CTH, whereas most arrows in the southeast are oriented southward, consistent with the RSH.

Downloaded from https://www.pnas.org by ETH Bibliothek on May 13, 2022 from IP address 129.132.180.126.

consistent with RSH. Fecundity and recruitment transitions amplify each other in the intermountain West. Taken together, the continental migration patterns align with regions where warming has been rapid (Fig. 3*A*), but driven by both fecundity and recruitment in the West, while dominated by recruitment in the East.

Discussion

The coherence of geographic shifts across a large number of species, tied to the specific demographic stages responsible for migration, adds insight to studies that rely solely on geographic centroids of abundance (34), centroids of tree growth rates (3, 22), or seedling abundances (7, 21, 30). The two processes, fecundity followed by recruitment, combine to produce biogeographic contrasts in net migration that are north–south rather than east–west; most northern species show poleward movement, while southern species show equator-ward displacement of recruitment (Fig. 4*E*). In the North, seedling recruitment is responding to climate warming faster than fecundity. On the one hand, it is important not to overinterpret the vector plots as a clean signal that migration can track rapid climate change. Even a species that is declining everywhere will have a geographic centroid somewhere. An arrow can point poleward, even if fecundity or recruitment is declining there, just so long as it is declining faster everywhere else. However, the coherence across species and regions (Fig. 4) offers the strongest support to date that migration is in progress with regional limitations on migration rate.

The geographic trends identified here are not dependent on assumptions of static forests prior to contemporary climate change. Subtle shifts in recent centuries predating contemporary climate change are known from at least some regions (e.g., ref. 48) and are expected from a range of processes related to climate variation, disturbance, and mortality events. By comparing the locations where seed production and recruitment are happening with the locations of adult trees (where recruitment happened decades to centuries ago), we identify how current recruitment differs from the generation that produced it.

In addition to migration, the analysis reveals previously undetected fecundity and recruitment hotspots in the Southeast and North, respectively (Fig. 3 *C* and *D*). The tree-to-recruit map of Fig. 4*E* hides the contributions of fecundity and seedling transitions, which can amplify or oppose one another (Fig. 3 *E* and *F*). Whether or not the extensive fecundity hotspot in the south-central continent (Fig. 3*C*) is related to high tree diversity there, this analysis establishes that it lies south of the main population centers for most species in that region (Fig. 3*E*). Fecundity is apparently not optimal near northern population frontiers in this region of slow warming, and, thus, it does not prime these populations for poleward spread. The fact that fecundity centers have not yet shifted northward of adult populations in the East could be expected both from limited warming in that region (Fig. 3*A*) and climate-sensitive seed production. Despite recruitment sensitivity in the East, the fact that the same region has experienced limited warming, combined with geographic contrasts identified here, suggests that migration in the East might accelerate with an increasing rate of warming.

The northern hotspot for recruitment (Fig. 3*D*) suggests that germination and early seedling survival may be more successful at northern frontiers than seed production. Whereas fecundity may be primed to lead tree migration in the West, local climate complexity that comes with rugged relief affects how migration potential should be interpreted. The combination of dry climates and fast climate change in the intermountain West explains fecundity and recruitment vectors in Fig. 3 *E* and *F* that point toward the cool, moist regional climates of the Northwest. However, for migration, these cool-moist conditions are locally found at higher elevations. The regional centroids average over this variation contributed by steep terrain.

The emergence of biogeographic trends related to climate change does not diminish the importance of local drainage, seed and seedling predators, pathogens, fire, and genetic diversity, all of which contribute variation to these maps. For example, fire contributes to recruitment beyond the direct effects of warming and drought (49, 50) and can directly regulate population frontiers (51). All mortality sources might contribute to spread through opening new sites for recruitment. Genetic diversity can contribute to biogeographic patterns through continuing adaptive responses (52, 53). Climate effects can be indirect through interactions with other variables (26, 54, 55). We lack the continental-scale coverage of these effects, but results here can help target species and regions for further study. More importantly, this analysis does not preclude effects of nonclimate variables or their interactions; rather, it exposes the relationships between fecundity and climate and geography, given that these other influences are also occurring.

Understanding how the biogeography of recruitment relates to patterns of species diversity, trait diversity, and forest structure emerges as a critical next goal for research and management. The biogeography of tree growth and forest structure mediates indirect climate effects across the continent. This analysis connects an eastern fecundity hotspot (Fig. 3*C*) to the continental trend toward young stands and fast-growing trees in this region (13). Regionally low fecundity in the West (Fig. 3*C*) relates to greater representation of larger, older trees that combine with rapid increase in temperature and moisture deficits. These coherent relationships between stand structure, composition, and climate provide a foundation for next steps toward the role of diversity and fertility gradients (55).

Adaptive management faces a global reforestation/afforestation challenge with species that can survive the rapid changes happening now and expected to continue for decades. If a fecundity drag on population spread in parts of the East contributes to centuries of lagging climate responses, then conservation and management may confront persistent disequilibrium with forest diversity and structure. These results for the role of fecundity and recruitment indicate that future planning efforts can benefit from knowledge of life-history stages and the species and genetic variants that are best able to tolerate future climate changes.

Materials and Methods

Fecundity Data. Fecundity data come from the MASTIF network (13), including longitudinal studies (Fig. 1*D*) and opportunistic sampling through the iNaturalist MASTIF project. The study includes 211K individual trees and 2.5M tree-years from 81 species. The model accommodates individual tree size, species, environment, and the codependence between trees and over time. It allows valid inference by accommodating the dependence in observations within trees over time and between trees, including quasisynchronous, quasiperiodic variation (47). The fitted model was then used to generate a predictive distribution of fecundity for each of 7.6M trees on 170K forest inventory plots across the United States and Canada.

We evaluated fecundity estimates per plot and, thus, per area. BA (m^2 /ha) of adult trees and new recruits into the smallest diameter class allowed us to determine fecundity as kg seed per m^2 BA and recruitment per kg seed, i.e., each of the transitions in Fig. 1*A*. Recruitment was evaluated from rates of ingrowth into inventory plots since 1999. Because fecundity cannot be aligned with ingrowth by year (there is a lag contributed by the seedling stage), we focus on time averages. Interannual variability can affect averages (56), but averages avoid the large uncertainty that would result from efforts to align annual fecundity and time-lagged recruitment. Covariates, sites, and species are summarized in more detail in *SI Appendix*.

Covariates. Covariates in the fecundity model include tree-level variables, including diameter and crown class (shading), and climate variables. A quadratic tree diameter term captures changes in diameters response with size (46). The shade classes in the model follow the Forest Inventory Analysis (FIA)/National Ecological Observation Network (NEON) scheme of 1 to 5, where 5 is a fully shaded canopy and 1 is a fully exposed canopy. Crown class is used in the model to provide information on competition.

Downloaded from https://www.pnas.org by ETH Bibliothek on May 13, 2022 from IP address 129.132.180.126.

Climate variables include spring minimum temperature (spring tmin, °C), summer mean temperature (summer tmean, °C), and moisture deficit (mm). Summer mean temperature (June through August), included as both a linear and quadratic term, is linked to thermal energy available during the growing season. Spring (March, April, and May) minimum temperature affects flowering and early fruit production. Finally, moisture deficit (cumulative monthly difference between potential evapotranspiration between January and August) is important for carbon assimilation and fruit development. To capture effects of spatial variation and interannual variability, climate variables were included as site means and site anomalies (26, 43). For species that develop over spring and summer, anomalies included the current and previous year. For species that disperse seeds in the spring (e.g., *Acer rubrum* and *Ulmus* species), only the previous year was used. Temperature anomalies were included for spring, but not summer, to reduce the number of temperature-related terms, as these two variables can be correlated. Variable selection for each species is detailed in ref. 47. Covariates were selected by variable selection (lowest deviance information criterion) (47). Climate variables were derived from gridded climate products and local climate-monitoring data where available, as described in *SI Appendix*.

Fecundity Inference. Standard modeling options, such as multivariate generalized linear regression models, do not address key features of the masting process. An observation consists of covariates (including tree attributes; *Covariates*) and responses for crop counts and seed traps. The maturation status of a tree (state at which a tree is able to produce seed), crop counts, and seed-trap data cannot be treated as independent data sources, as each is linked to the same tree. Because fecundity is quasiperiodic and quasisynchronous, all trees and years must be modeled jointly.

The MASTIF model (47) exploits conditional independence to accommodate dependence between trees and within trees over years. Latent variables for maturation state and tree-year seed production are part of the posterior distribution. Posterior simulation of parameters and latent states is accomplished with Markov chain Monte Carlo, direct (Gibbs) sampling, and Hamiltonian Markov Chain updates. The structure and methodology is implemented in the R package Mast Inference and Forecasting. Partial autocorrelation functions quantify the contribution of each lag *p*, detailed in ref. 47.

Tree Inventories and Fecundity Prediction. Abundance and recruitment were estimated from multiple forest inventories, including the US Department of Agriculture FIA, NEON, the Canadian National Forest Inventory (CNFI), and the MASTIF network of sites. Predictive distributions for individual tree fecundity combine the fitted model with tree-level observations of species, diameter, crown class, and climate variables (*Covariates*) from these inventories. For both fecundity and inventory data, climate norms were taken from 1990 to 2019. Fecundity prediction was applied to 7,723,671 trees on inventory plots, including FIA, CNFI, NEON, and MASTIF. Mean estimates for the genus were used for inventory trees belonging to species for which there were not confident fits in the MASTIF model, which amounted to 7.2% of inventory trees. Predictive distributions were computed for plots with abundance and recruitment data.

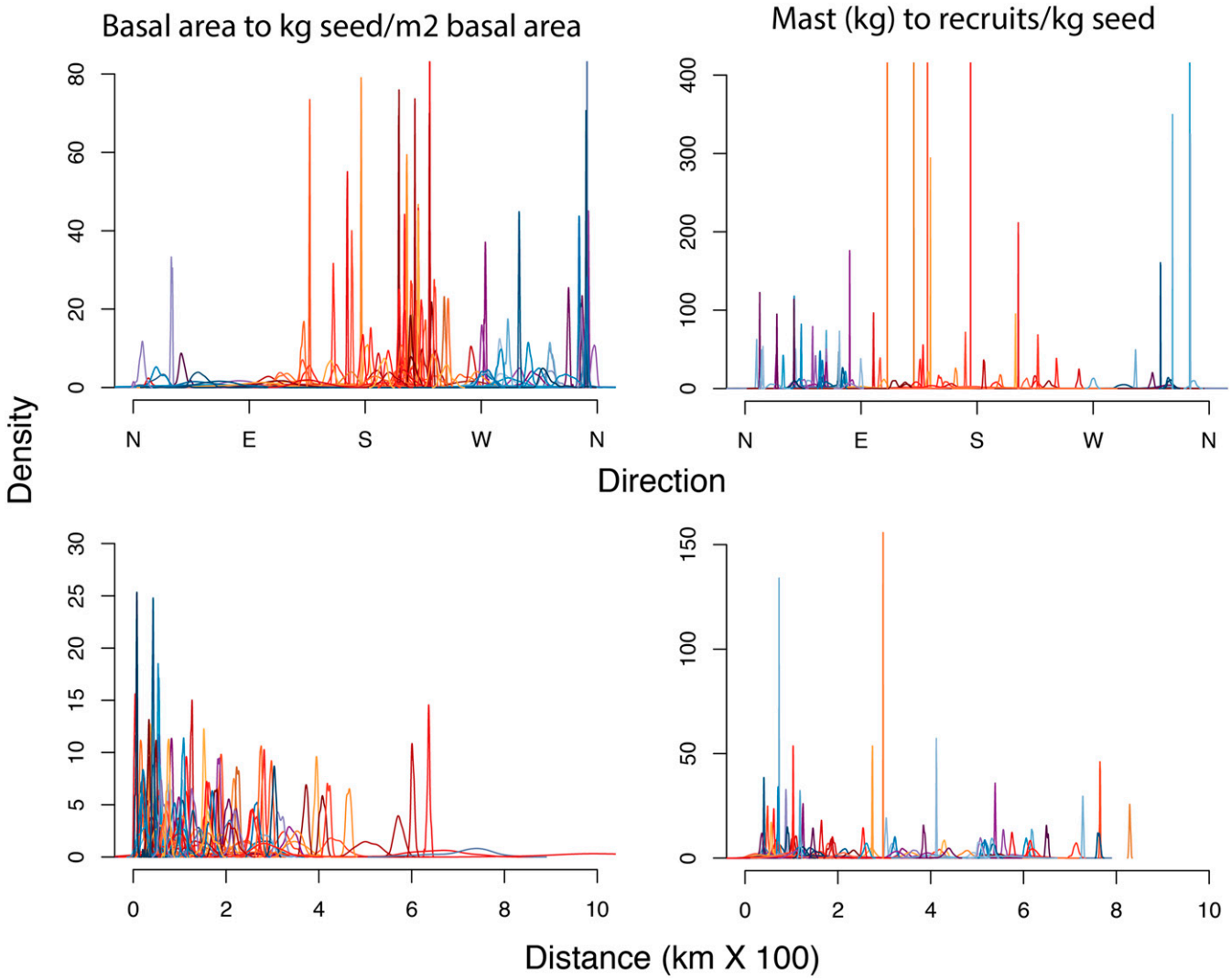

Fig. 5. Uncertainty in vector fields. Predictive distributions (drawn from the posterior) for map vectors in Fig. 3 *E* (*Left*) and 3 *F* (*Right*), as applied to every tree in inventory data. Each posterior is one species color coded for vectors where the mode is oriented south (reds) and north (blues).

Downloaded from https://www.pnas.org by ETH Bibliothek on May 13, 2022 from IP address 129.132.180.126.

For recruitment, we evaluated ingrowth to plots as recruits $ha^{-1} \cdot y^{-1}$ in FIA, the CNFI, and the longitudinal sites that include seed-trap data (*SI Appendix*, Table S2.2). For FIA, we included remeasured plots after the standard national protocol was implemented in 1999. Plots with less than 25% forest cover were omitted, because this variable can indicate human disturbance. The RECONCILECD code = 1 indicates an ingrowth tree. The diameter threshold for ingrowth trees is from 1 to 5 in diameter at breast height (dbh). New trees introduced into inventory plots that were untagged or accidentally skipped in last inventory were not included in the analysis. Estimated recruits per year was evaluated as the number of recruits divided by the duration of the interval (the REMPER [or "remeasurement period"] variable) and scaled by their area representation, which depends on plot size. For CNFI, ingrowth included trees that appeared in a sample for the first time. The minimum diameter for CNFI plots is 9 cm. For consistency between inventories, we evaluated ingrowth at 12 cm dbh.

Habitat Suitability Change. The shift in habitat suitability for an example species in Fig. 2 provides the sense of geographic scale that is required for tracking contemporary climate change. *P. taeda* was used for this example because it is abundant and well-predicted by climate and habitat variables, and its range is entirely within the Southeast, so that responses to habitat suitability change could be displayed on the map for the study region (the continental United States in Fig. 2*B*). *P. taeda* is managed for forest products, but primarily within its historic range limits (see also ref. 57).

As one of several approaches used to infer and predict geographic change in habitat suitability, Generalized Joint Attribution Modeling (GJAM) accommodates the joint distribution of species and the zero dominance of BA data. As is typical for forest inventory data, BA for most species at most locations is zero. This point mass at zero must be assimilated with continuous variation in BA for all nonzero values. Methods are detailed in ref. 58 with a full catalog of species at Predicting Biodiversity with GJAM. Another extensive catalog based on univariate models is available from the Climate Change Atlas. Covariates for the analysis in Fig. 2 include mean annual temperature (°C), annual moisture deficit *D* (mm), elevation (m), clay content (%), soil depth (cm), and slope.

Centroids and Vector Fields. The geographic centroids for BA, fecundity, and recruitment in Figs. 3 *E* and *F* and 4*E* are weighted average locations (latitude, longitude),

$$\bar{x} = \frac{\sum_i w_i x_i}{\sum_i w_i}, \qquad [1]$$

where x_i is latitude or longitude of an observation i, w_i is the weight (BA, fecundity, or recruitment), and $\bar{x}$ is the latitude or longitude centroid. Likewise, the climate centroids in Fig. 4 *C* and *D* are weighted averages in climate space, where x_i in the previous equation is replaced with a climate variable. Arrows on maps are drawn from geographic centroids of one variable (e.g., tree BA or fecundity) to another (e.g., fecundity or recruitment).

Because uncertainty in the vector fields of Fig. 3 *E* and *F* could not be transparently displayed in the same maps, their densities are shown in Fig. 5 for distance and direction. Posterior estimates of seed production for each tree determine the distribution of centroids using Eq. **1** through Monte Carlo integration. In Fig. 3*E*, the vector origins are determined by tree BA from the inventory data, and vector weights in Eq. **1** are random, given by the posterior distribution for tree fecundities (kg seed per m^2 BA). In Fig. 3*F*, vector origins are random, determined by the posterior distribution of fecundities, with vector weights determined by recruits per kg seed. The highly resolved densities for vector direction and distance in Fig. 5 come from the fact that, like an SE, the posterior width declines with the square root of sample size, and sample sizes in this study are large.

Rose Plots. Rose plots in Fig. 4 show distance-weighted circular averages (black arrows) for the displacements between BA and fecundity and between fecundity and recruitment, computed as

$$\bar{\alpha} = \arctan\left(\frac{1}{n}\sum_{j=1}^{n} w_j \sin\alpha_j, \frac{1}{n}\sum_{j=1}^{n} w_j \cos\alpha_j\right),$$

where $\bar{\alpha}$ is the distance weighted circular average, w_j is relative distance weight (length of arrow *j*), and α_j is the vector angle in radians.

Data Availability. Seed production data have been deposited in the Duke Data Repository (https://doi.org/10.7924/r4348ph5t) (59).

ACKNOWLEDGMENTS. For access to sites and logistical support, we thank NEON. For comments on the manuscript, we thank S. Higgins, V. Journé, R. Palacio, and T. Qiu. The project was supported by NSF Grant DEB-1754443; Belmont Forum Grant 1854976; NASA Grants AIST16-0052 and AIST18-0063; and Programme d'Investissement d'Avenir Project Forecasting Biodiversity Change Grant 18-MPGA-0004. Any use of trade, firm, or product names is for descriptive purposes only and does not imply endorsement by the US Government.

1. R. Hickling, D. Roy, J. Hill, R. Fox, C. Thomas, The distributions of a wide range of taxonomic groups are expanding polewards. *Glob. Change Biol.* **12**, 450–455 (2006).
2. L. Boisvert-Marsh, C. Périé, S. de Blois, Shifting with climate? Evidence for recent changes in tree species distribution at high latitudes. *Ecosphere* **5**, 1–33 (2014).
3. K. J. Feeley *et al.*, Upslope migration of Andean trees. *J. Biogeogr.* **38**, 783–791 (2011).
4. M. Gottfried *et al.*, Continent-wide response of mountain vegetation to climate change. *Nat. Clim. Chang.* **2**, 111–115 (2012).
5. J. S. Clark, M. Lewis, J. S. McLachlan, J. HilleRisLambers, Estimating population spread: What can we forecast and how well? *Ecology* **84**, 1979–1988 (2003).
6. R. K. Danby, D. S. Hik, Evidence of recent treeline dynamics in southwest Yukon from aerial photographs. *Arctic* **60**, 411–420 (2007).
7. C. W. Woodall *et al.*, An indicator of tree migration in forests of the eastern United States. *For. Ecol. Manage.* **257**, 1434–1444 (2009).
8. S. W. Flake, P. J. Weisberg, Widespread mortality and defoliation of pinyon pine in central Nevada mountains. *Bull. Ecol. Soc. Am.* **100**, e01507 (2019).
9. E. Liang *et al.*, Species interactions slow warming-induced upward shifts of treelines on the Tibetan Plateau. *Proc. Natl. Acad. Sci. U.S.A.* **113**, 4380–4385 (2016).
10. R. Cazzolla Gatti *et al.*, Accelerating upward treeline shift in the Altai Mountains under last-century climate change. *Sci. Rep.* **9**, 7678 (2019).
11. H. Lischke, N. Zimmermann, J. Bolliger, S. Rickebusch, T. Löffler, TreeMig: A forest-landscape model for simulating spatio-temporal patterns from stand to landscape scale. *Ecol. Modell.* **199**, 409–420 (2006).
12. N. G. McDowell *et al.*, Pervasive shifts in forest dynamics in a changing world. *Science* **368**, eaaz9463 (2020).
13. J. S. Clark *et al.*, Continent-wide tree fecundity driven by indirect climate effects. *Nat. Commun.* **12**, 1242 (2021).
14. M. C. Urban, Climate change. Accelerating extinction risk from climate change. *Science* **348**, 571–573 (2015).
15. S. Zolkos *et al.*, Projected tree species redistribution under climate change: Implications for ecosystem vulnerability across protected areas in the eastern United States. *Ecosystems (N. Y.)* **18**, 202–220 (2015).
16. C. I. Millar, N. L. Stephenson, Temperate forest health in an era of emerging megadisturbance. *Science* **349**, 823–826 (2015).
17. D. M. P. Moorcroft, Tree mortality in the eastern and central U.S.: Patterns and drivers. *Glob. Change Biol.* **17**, 3312–3326 (2011).
18. C. D. Allen, D. D. Breshears, N. G. McDowell, On underestimation of global vulnerability to tree mortality and forest die-off from hotter drought in the Anthropocene. *Ecosphere* **6**, 1–55 (2015).
19. A. P. Williams *et al.*, Large contribution from anthropogenic warming to an emerging North American megadrought. *Science* **368**, 314–318 (2020).
20. I. Ibanez, J. S. Clark, M. C. Dietze, Estimating colonization potential of migrant tree species. *Glob. Change Biol.* **15**, 1173–1188 (2009).
21. K. Zhu, C. W. Woodall, J. S. Clark, Failure to migrate: Lack of tree range expansion in response to climate change. *Glob. Change Biol.* **18**, 1042–1052 (2011).
22. K. J. Feeley, E. M. Rehm, B. Machovina, The responses of tropical forest species to global climate change: Acclimate, adapt, migrate, or go extinct? *Front. Biogeogr.* **4**, fb_12621 (2012).
23. D. M. Bell, J. B. Bradford, W. K. Lauenroth, Early indicators of change: Divergent climate envelopes between tree life stages imply range shifts in the western United States. *Glob. Ecol. Biogeogr.* **23**, 168–180 (2014).
24. C. W. Woodall, D. J. Nowak, G. C. Liknes, J. A. Westfall, Assessing the potential for urban trees to facilitate forest tree migration in the eastern United States. *For. Ecol. Manage.* **259**, 1447–1454 (2010).
25. F. Sittaro, A. Paquette, C. Messier, C. A. Nock, Tree range expansion in eastern North America fails to keep pace with climate warming at northern range limits. *Glob. Change Biol.* **23**, 3292–3301 (2017).
26. J. S. Clark, D. M. Bell, M. C. Kwit, K. Zhu, Competition-interaction landscapes for the joint response of forests to climate change. *Glob. Change Biol.* **20**, 1979–1991 (2014).
27. D. M. Bell, J. B. Bradford, W. K. Lauenroth, Mountain landscapes offer few opportunities for high-elevation tree species migration. *Glob. Change Biol.* **20**, 1441–1451 (2014).
28. J. M. Tylianakis, R. K. Didham, J. Bascompte, D. A. Wardle, Global change and species interactions in terrestrial ecosystems. *Ecol. Lett.* **11**, 1351–1363 (2008).
29. I. Ibáñez, D. S. W. Katz, B. R. Lee, The contrasting effects of short-term climate change on the early recruitment of tree species. *Oecologia* **184**, 701–713 (2017).
30. V. J. Monleon, H. E. Lintz, Evidence of tree species' range shifts in a complex landscape. *PLoS One* **10**, e0118069 (2015).
31. P. L. Marks, S. Gardescu, A case study of sugar maple (*Acer saccharum*) as a forest seedling bank species. *J. Torrey Bot. Soc.* **125**, 287–296 (1998).
32. J. A. Antos, H. J. Guest, R. Parish, The tree seedling bank in an ancient montane forest: Stress tolerators in a productive habitat. *J. Ecol.* **93**, 536–543 (2005).
33. K. Zhu, C. W. Woodall, J. V. Monteiro, J. S. Clark, Prevalence and strength of density-dependent tree recruitment. *Ecology* **96**, 2319–2327 (2015).
34. S. Fei *et al.*, Divergence of species responses to climate change. *Sci. Adv.* **3**, e1603055 (2017).

Downloaded from https://www.pnas.org by ETH Bibliothek on May 13, 2022 from IP address 129.132.180.126.

35. J. Guldin, Silvicultural options in forests of the southern United States under changing climatic conditions. *New For.* **50**, 1–17 (2018).
36. F. Máliš *et al.*, Life stage, not climate change, explains observed tree range shifts. *Glob. Change Biol.* **22**, 1904–1914 (2016).
37. J. S. Clark *et al.*, The impacts of increasing drought on forest dynamics, structure, and biodiversity in the United States. *Glob. Change Biol.* **22**, 2329–2352 (2016).
38. B. R. Murray, A. H. D. Brown, C. R. Dickman, M. S. Crowther, Geographical gradients in seed mass in relation to climate. *J. Biogeogr.* **31**, 379–388 (2004).
39. A. Moles, D. Falster, M. Leishman, M. Westoby, Small-seeded species produce more seeds per square metre of canopy per year, but not per individual per lifetime. *J. Ecol.* **92**, 384–396 (2004).
40. R. J. Aicher, L. Larios, K. N. Suding, Seed supply, recruitment, and assembly: Quantifying relative seed and establishment limitation in a plant community context. *Am. Nat.* **178**, 464–477 (2011).
41. R. García-Camacho, J. M. Iriondo, A. Escudero, Seedling dynamics at elevation limits: Complex interactions beyond seed and microsite limitations. *Am. J. Bot.* **97**, 1791–1797 (2010).
42. A. Jönsson, A. Linderson, I. Stjernquist, P. Schlyter, L. Bärring, Climate change and the effect of temperature backlashes causing frost damage in *Picea abies*. *Global Planet. Change* **44**, 195–207 (2004).
43. J. S. Clark, D. Bell, M. Hersh, L. Nichols, Climate change vulnerability of forest biodiversity: Climate and competition tracking of demographic rates. *Glob. Change Biol.* **17**, 1834–1849 (2011).
44. C. Kollas, C. Körner, C. Randin, Spring frost and growing season length co-control the cold range limits of broad-leaved trees. *J. Biogeogr.* **41**, 773–783 (2014).
45. S. M. Vicente-Serrano, S. Beguería, J. I. López-Moreno, A multiscalar drought index sensitive to global warming: The standardized precipitation evapotranspiration index. *J. Clim.* **23**, 1696–1718 (2010).
46. T. Qiu *et al.*, Is there tree senescence? The fecundity evidence. *Proc. Natl. Acad. Sci. U.S.A.* **118**, 1–10 (2021).
47. J. S. Clark, C. Nunez, B. Tomasek, Foodwebs based on unreliable foundations: Spatiotemporal masting merged with consumer movement, storage, and diet. *Ecol. Monogr.* **89**, e01381 (2019).
48. A. Dawson *et al.*, Quantifying trends and uncertainty in prehistoric forest composition in the upper Midwestern United States. *Ecology* **100**, e02856 (2019).
49. C. Brown, J. Johnstone, Once burned, twice shy: Repeat fires reduce seed availability and alter substrate constraints on picea mariana regeneration. *For. Ecol. Manage.* **266**, 34–41 (2012).
50. L. Burkle, J. Myers, R. Belote, Wildfire disturbance and productivity as drivers of plant species diversity across spatial scales. *Ecosphere* **6**, art202 (2015).
51. B. Rayfield *et al.*, Influence of habitat availability and fire disturbance on a northern range boundary. *J. Biogeogr.*, 10.1111/jbi.14004 (2020).
52. H. F. Cooper *et al.*, Genotypic variation in phenological plasticity: Reciprocal common gardens reveal adaptive responses to warmer springs but not to fall frost. *Glob. Change Biol.* **25**, 187–200 (2019).
53. T. G. Whitham, G. J. Allan, H. F. Cooper, S. M. Shuster, Intraspecific genetic variation and species interactions contribute to community evolution. *Annu. Rev. Ecol. Evol. Syst.* **51**, 587–612 (2020).
54. I. Visnadi *et al.*, Limited recruitment of eastern white cedar (*Thuja occidentalis* L.) under black spruce canopy at its northern distribution limit. *Ecoscience* **26**, 123–132 (2019).
55. B. Seyednasrollah, J. S. Clark, Where resource-acquisitive species are located: The role of habitat heterogeneity. *Geophys. Res. Lett.* **47**, e2020GL087626 (2020).
56. M. Bogdziewicz, M. Fernández-Martínez, J. Espelta, R. Ogaya, J. Penuelas, Is forest fecundity resistant to drought? Results from an 18-yr rainfall-reduction experiment. *New Phytol.* **227**, 1073–1080 (2020).
57. L. R. Iverson, M. P. Peters, A. M. Prasad, S. N. Matthews, Analysis of climate change impacts on tree species of the eastern US: Results of DISTRIB-II modeling. *Forests* **10**, 302 (2019).
58. J. S. Clark, D. Nemergut, B. Seyednasrollah, P. J. Turner, S. Zhang, Generalized joint attribute modeling for biodiversity analysis: Median-zero, multivariate, multifarious data. *Ecol. Monogr.* **87**, 34–56 (2017).
59. J. S. Clark, Data from: Continent-wide tree fecundity driven by indirect climate effects. Duke Research Data Repository. https://doi.org/10.7924/r4348ph5t. Deposited 8 October 2020.

Downloaded from https://www.pnas.org by ETH Bibliothek on May 13, 2022 from IP address 129.132.180.126.